

# Ripple Reduction of BLDC using Direct Torque Control

D. Sivaraj<sup>1</sup>, R.Goutham Govind Raju<sup>2</sup>, S.Anandakumar<sup>3</sup>, L.Selvakumar<sup>4</sup>

Assistant Professor, Dept. of Electrical and Electronics Engg., Christ college of Engg., & Technology<sup>1,2,3,4</sup>

**Abstract:** Brushless DC motor has a rotor with permanent magnet and has no mechanical commutator which leads to many advantages like less maintenance, long life, high reliability, low inertia, low friction and low noise. Since the brush system/commutator assembly is replaced by an electronic controller which can be easily integrated into other required electronics, thereby improving the effective power to weight and power to volume ratio. To minimize the torque ripple using conventional current controller and the direct torque controller in BLDC motor using SIMULINK and to verify the results by simulation. In this paper the direct torque control method is employed to improve its torque ripple content which is been compared with conventional method by using MATLAB software and the result where comprehensively presented through extensive simulations which shows successfully mitigating almost 50% of ripple.

**Keywords:** DTC, BLDC, ripple, Hall Effect, current controller.

## I INTRODUCTION

BLDC motor has trapezoidal back-EMF waveform in order to minimize the torque ripple and maximize the efficiency and torque capability. A sinusoidal back-EMF waveform can be obtained by skewing the stator slots and/or rotor magnets, employing a distributed stator winding, shaping the magnets, or employing a sinusoidal magnetization distribution. BLDC motors often employ concentrated windings, since these results in shorter end windings, which is conducive to a high efficiency and torque density[1-5].

Generally, BLDC drives employ current control, which essentially assumes that the torque is proportional to the phase current. Since, in practice, the relationship is nonlinear, various current control strategies have been adopted to minimize torque pulsations which resulted in minimal copper loss and ripple-free torque from a BLDC drive. However, it was based on the d-q axes transformation, and could not respond to rapid torque changes[5-9]. A current controller is used to estimate the electromagnetic torque from the rate of change of co energy. In DTC of BLDC drive, the estimated torque was obtained from a lookup table, and the control algorithm did not directly involve flux control. Electromagnetic torque pulsations were reduced with a torque controller in which the torque was estimated from the product of the instantaneous back-EMF and current [10-15]

Direct torque control (DTC) is defined as directly control of the flux linkage and electromagnetic torque. Considering the electrical machine, the power electronic inverter, and the control strategy at the system level, a relationship is established between the torque, the flux and the optimal inverter switching so as to achieve a fast torque response[16-17]. It exhibits better dynamic performance than conventional control methods, such as vector control, is less sensitive to parameter variations, and is simpler to implement on BLDC motor using 120° conduction mode (i.e. Two phases conducting) to achieve instantaneous torque control and reduced torque ripple [18-20]

This paper is organized as follows, in section II detail principle of operation of BLDC motor where presented. In section III an implementation of conventional current control in Brushless DC motor is explained, in section IV provides the implementation of direct torque control in Brushless DC Motor, finally in section V simulation results of conventional current control and direct torque Control of Brushless DC Motor. And at the end conclusions were given.

## II OPERATION

The BLDC motors have many advantages over brushed DC motor and induction motor drives, which are not only 'brushless' but make use of 'standard' motors. In the same frame, with the same cooling, the brushless DC motor will have better efficiency, power factor, and better speed-torque characteristics, high dynamic response, long operating life, noiseless operation and higher speed ranges.

### A. Six - Step Commutation

The conducting interval for each phase is 120° electrical angle. The commutation phase sequence is like AB-AC-BC-BA-CA-CB, where A, B, C are the three phases. Each conducting stage is called one step. Therefore, only two phases conduct current at any time, leaving the third phase floating. In order to produce maximum torque, the inverter should be commutated every 60° so that current is in phase with the back EMF which is explained in figure 1. The commutation timing is determined by the rotor position, which can be detected by position sensors.

### A Back EMF

When a BLDC motor rotates, each winding generates a voltage known as back Electromotive Force or back EMF, which opposes the main voltage supplied to the windings according to Lenz's Law. The polarity of this back EMF is in opposite direction of the energized voltage. Back EMF depends mainly on three factors:

- Angular velocity of the rotor
- Magnetic field generated by rotor magnets
- The number of turns in the stator windings

Back EMF,

$$E \propto NlrB\omega \quad (1)$$

Where:

$N$  is the number of winding turns per phase,  
 $l$  is the length of the rotor,  
 $r$  is the internal radius of the rotor,  
 $B$  is the rotor magnetic field density and  
 $\omega$  is the motor's angular velocity.

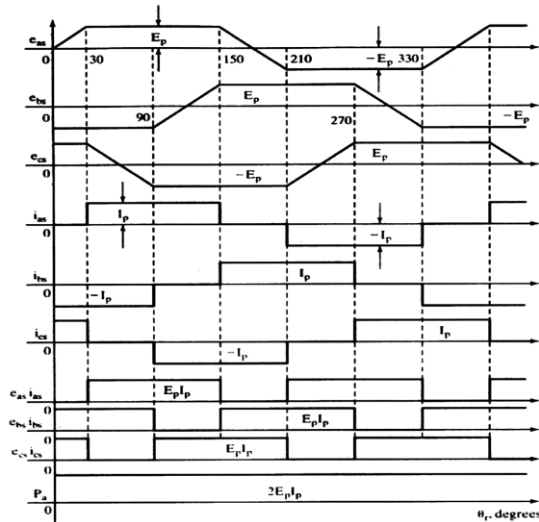


Fig 1: PM Brushless DC Motor waveforms

Once the motor is designed, the rotor magnetic field and the number of turns in the stator windings remain constant. The only factor that governs back EMF is the angular velocity or speed of the rotor and as the speed increases, back EMF also increases. The motor technical specification gives a parameter called, back EMF constant, that can be used to estimate back EMF for a given speed.

### III CURRENT CONTROL OF BLDC MOTOR

The conventional current control, by properly selecting the inverter voltage space vectors of the two phase conduction mode from a simple look-up table at a predefined sampling time, the described square wave current is obtained. Therefore a much faster torque response is achieved in the current control technique.

The speed controller is based on a PI regulator, shown below. The output of this regulator is a torque set point applied to the current controller block. For constant torque operation at speeds lower than the base speed, this drive requires six discrete pieces of position information. They correspond to every 60 electrical degrees for energizing the three stator phases, the control scheme for the BLDC drive is simple and is shown in figure 2.

The resolver gives absolute rotor position; it is converted in to rotor speed through the signal processor. The rotor speed is compared to its reference, and the rotor speed error is amplified through the speed controller. The output of the speed controller provides the reference torque.

$$T_e^* = \lambda_p [f_{as}(\theta_r)i_{as}^* + f_{bs}(\theta_r)i_{bs}^* + f_{cs}(\theta_r)i_{cs}^*] \quad (3.1)$$

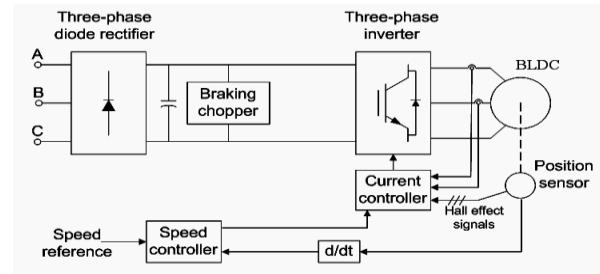


Fig 2: block diagram of current control BLDC

Only two phases conduct current at any time, with the two phases being in series for full-wave inverter operation. So the phase currents are equal in magnitude but opposite sign. The rotor position-dependent functions have the same signs as the stator phase currents in the motoring mode, but opposite sign in the regeneration mode.

$$T_e^* = 2\lambda_p i_p^* \quad (3.2)$$

The stator-current command is derived from

$$i_p^* = T_e^* / 2\lambda_p \quad (3.3)$$

The individual stator phase-current commands are generated from the current-magnitude command and absolute rotor position. These current commands are amplified through the inverter by comparing them with their respective currents in the stator phases. Only two phases current are necessary in the balanced three-phase system to obtain the third phase current. Since the sum of the three phase currents is zero.

The currents errors are amplified and used with pulse with modulation or hysteresis logic to produce the switching-logic signals for the inverter switches.

#### A Speed controller

In closed loop speed control the actual speed is measured and compared with the reference speed to find the error difference. This error difference will be supplied to the PI controller. The output from the PI controller gives the desired torque. The speed controller is based on a PI regulator, shown in figure 3. The output of this regulator is a torque set point applied to the current controller block.

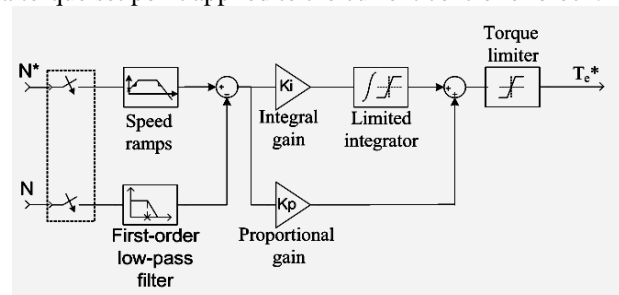


Fig 3: Design of Speed Controller

#### B Current control

At least two phase currents are required for the current control of three phase machines. The phase currents can be sensed from the dc link current. Hence, one sensor is sufficient for current control of the machine the current sensors are relatively expensive if galvanic isolation is required.

Hall Effect current sensors are ideal for sensing the currents with galvanic isolation. At this stage, it is very nearly impossible to do away with current feedbacks for

the control of the PMSM machine to deliver high performance. If precise torque and speed controls are not required, current feedback control and hence current sensing can be dispensed with. Then, a simple duty cycle using an open-loop PWM voltage controller is sufficient. However, the steering of the current to the appropriate machine phases requires the rotor-position information. A number of methods have come in to practice to estimate rotor position information without an externally mounted sensor as shown in figure 4.

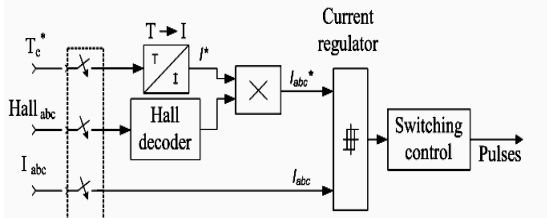


Fig 4: Design of Current Controller

#### IV DIRECT TORQUE CONTROL SCHEME

The direct torque control (DTC) directly controls the inverter states based on the errors between the reference and estimated values of torque and flux. It selects one of six voltage vectors generated by a voltage source inverter to keep torque and flux within limits of two hysteresis bands. Characteristics of DTC are: Good dynamic torque response, Robustness, Low complexity

##### A Three Phase Inverter

Consider a three-phase inverter shown in figure 6, Q1 through Q6 are the six power transistors that shape the output current, which are controlled by the switching signals a, a', b, b', c and c'. When an upper transistor is switched on, the corresponding lower transistor is switched off. Hence, the three-phase inverter can produce eight output states. Switching state 100 means, upper switch in phase a is closed, and upper switches in phase b and c are open. For each of the possible switching states, thus, eight output states of inverter represent eight space vectors; two are null vectors and remaining six are of equal magnitude and arranged 60° apart in space. The space diagram is shown in the Figure 5

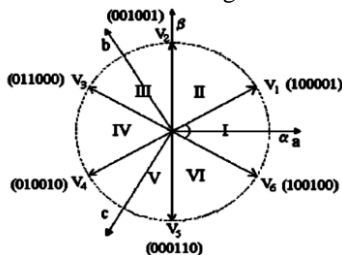


Fig 5: sector selection

##### B Concept of Direct Torque Control

The block diagram for direct torque and flux control is shown in figure 6. The command stator flux reference is generated by the speed to flux look up table and the command torque reference is generated by the speed controller which converts speed error into torque. Torque and flux are estimated by taking motor line voltages and currents. After transforming these three phase components into two phase stationary components stator flux, torque and angle in which the stator flux lies are estimated

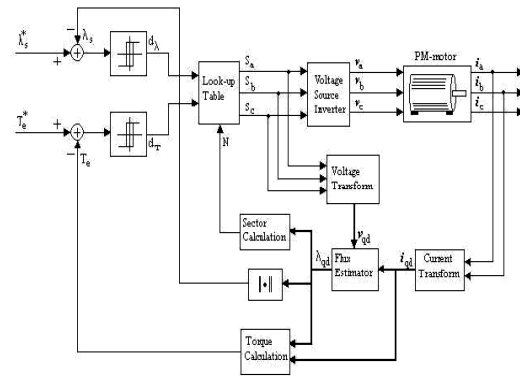


Fig 6: block diagram of DTC system

The reference flux and torque commands are compared with the estimated values and the errors are processed through hysteresis-band controllers. Selection of the appropriate voltage vector in the inverter is based on stator equation in stator coordinates.

##### C Direct Torque Control of Brushless Dc Motor

The rotor flux linkage in the stationary reference frame can be calculated from (4.7) and (4.8), while the magnitude of the stator flux linkage and the electromagnetic torque can be obtained from (4.3),(4.4) and (4.2), respectively. The speed feedback derived from rotor position sensors is compared to the speed command to form the torque command from the proportional – integral (PI) speed regulator. The stator flux-linkage and torque commands are obtained from hysteresis controllers by comparing the estimated electromagnetic torque and stator flux linkage with their demanded values. As can be seen from Table I, the switching pattern of the inverter can be determined according to the stator flux-linkage and torque status from the outputs of two regulators shown in figure 7 and the sector in which the stator flux linkage is located at that instant of time.

In general, neglecting the influence of mutual coupling between the direct and quadrature axes, the electromagnetic torque of a permanent-magnet brushless dc machine can be expressed as

$$T_e = \frac{3}{2} \frac{p}{2} \left[ \left( \frac{d\psi_{rd}}{d\theta_e} - \psi_{rq} \right) i_{sd} + \left( \frac{d\psi_{rq}}{d\theta_e} - \psi_{rd} \right) i_{sq} \right] \quad (4.1)$$

For non sinusoidal stator flux linkage, since  $L_{d0}=L_{q0}=L_s$ , the electromagnetic torque, for both BLDC and BLDC operation, can be simplified as,

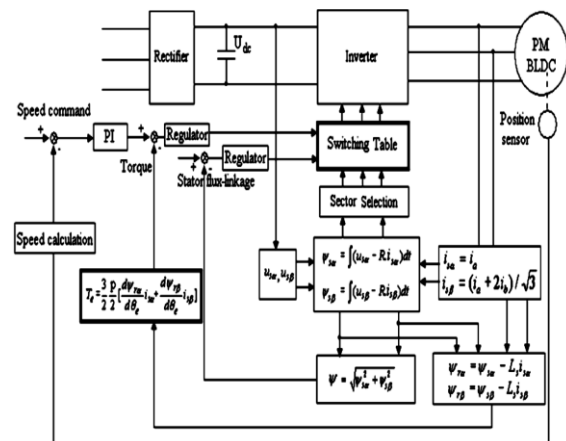


Fig 7: schematic of a DTC brushless dc motor

$$T_e = \frac{3}{2} \frac{p}{2} \left[ \frac{d\psi_{r\alpha}}{d\theta_e} i_{s\alpha} + \frac{d\psi_{r\beta}}{d\theta_e} i_{s\beta} \right] \quad (4.2)$$

DTC strategy of BLDC drives is based on the flux linkage observers. The stator flux-linkage vector can be obtained from the measured stator voltages,  $u_s$ , and current  $i_s$ . The magnitude and position of the stator flux linkage can be calculated, respectively. The electromagnetic torque equation for a BLDC motor can be expressed in terms of rotor flux linkages, where  $\psi_{r\alpha}$  and  $\psi_{r\beta}$  are the  $\alpha$ - and  $\beta$ -axes rotor flux linkages, The stator flux-linkage vector can be obtained from the measured stator voltages  $U_{s\alpha}$  and  $U_{s\beta}$  and currents  $i_{s\alpha}$  and  $i_{s\beta}$  as

$$\psi_{s\alpha} = \int (u_{s\alpha} - R i_{s\alpha}) dt \quad (4.3)$$

$$\psi_{s\beta} = \int (u_{s\beta} - R i_{s\beta}) dt \quad (4.4)$$

Where  $R$  is the stator winding resistance. The magnitude and angular position of the stator flux-linkage vector is obtained as

$$\psi = \sqrt{\psi_{s\alpha}^2 + \psi_{s\beta}^2} \quad (4.5)$$

$$\theta = \arctan \frac{\psi_{s\beta}}{\psi_{s\alpha}} \quad (4.6)$$

The rotor flux linkages can be deduced from the stator flux linkages

$$\psi_{r\alpha} = \psi_{s\alpha} - L_s i_{s\alpha} \quad (4.7)$$

$$\psi_{r\beta} = \psi_{s\beta} - L_s i_{s\beta} \quad (4.8)$$

While the torque can be calculated from (4.2) to simplify the calculation, however, the differential terms in (4.1) can be pre-determined from the back-EMF waveform assuming that the EMF is proportional to the rotor speed. Six nonzero-voltage space vectors are defined for a BLDC drive as shown in figure 8. And their relationship with the voltage space-vector sectors and switching states. The idealized phase current waveform for BLDC drives is shown in figure 9.

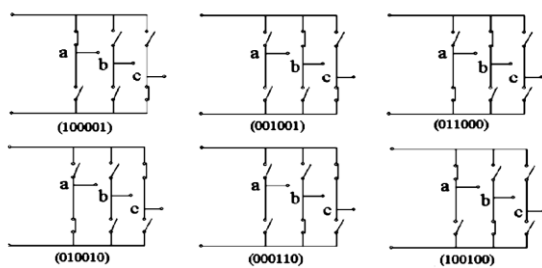


Fig 8: Non-zero voltage space vector selection of switches

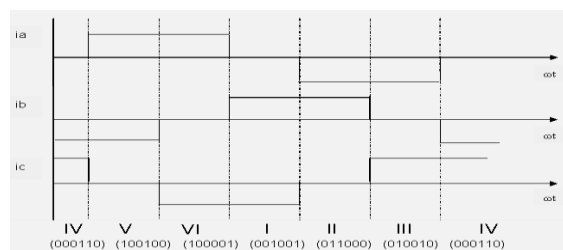


Fig 9: Idealized phase current

In a BLDC drive, all three phases are conducting at any instant and the voltage space vectors can be represented by three digits which fully represent all the states of the inverter switches, since only one digit is

required for each switching leg, as the upper and lower switches operate in tandem mode. In a BLDC drive, however, only two phases are conducting in the 120 conduction mode, except during commutation periods when all three phases conduct, the unexcited phase conducting via a freewheeling diode.

Since the upper and lower switches in the same phase leg may both be simultaneously off in BLDC drive, irrespective of the state of the associated freewheel diodes six digits are required to represent the states of the inverter switches, one digit for each switch. Thus, the voltage space vectors  $V_1, V_2 \dots V_6$  are represented as switching signals (100 001), (001 001), (011 000), (010 010), (000 110), (100 100), respectively, where, From left to right, the logical values express the states of the upper and lower switching Signals for phases A, B and C respectively. The zero-voltage space vector is defined as (000000). The voltage space vectors in the  $d-q$  reference frame for a BLDC drive have a 30 phase difference relative to those for a BLDC drive.

## V SIMULATION RESULTS

The model of the brushless DC motor drive system is simulated to investigate its dynamic performance and simulated results are shown in this chapter. The motor parameters used for simulation are given in appendix. The motor performance is tested under conventional current control and direct torque control.

Comparative result of three phase current for both conventional current control and Direct torque control are explained at 400 rpm and at 1Nm in which motor phase currents (a, b, c) shown in Figure 10 (a) and (b).

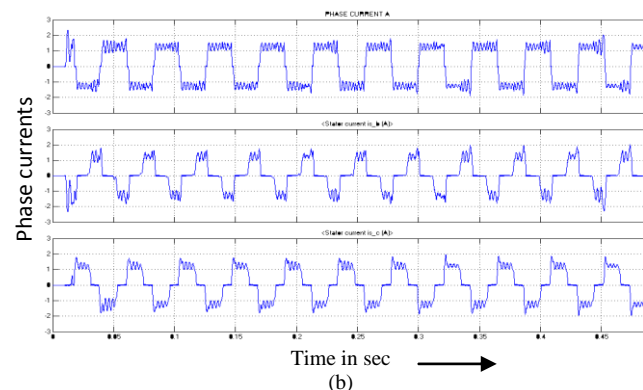
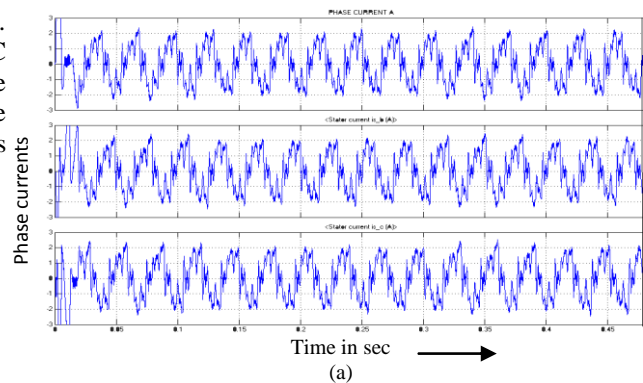


Fig 10: Three phase current of BLDC motor using Direct Torque Control At rated speed (400 rpm),  $T_L=1Nm$ .

Figure 11 (a) and (b) shows the Comparative result of three phase Back EMF for both conventional current Control and Direct torque control BLDC

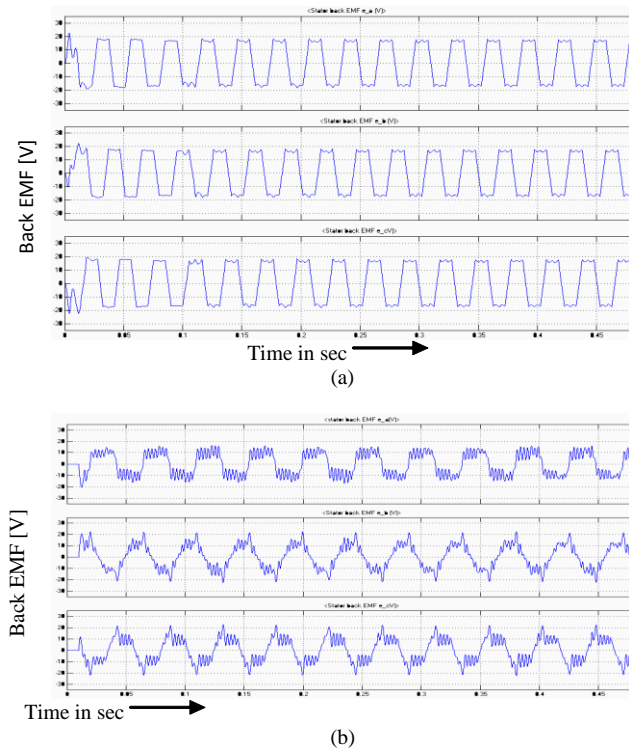


Fig 11: Three phase Back EMF of BLDC motor using Direct Torque Control At rated speed (400 rpm), TL=1Nm.

Figure 12 (a) and (b) show the Comparative Result of the electromagnetic torque for both conventional current Control and Direct torque control BLDC.

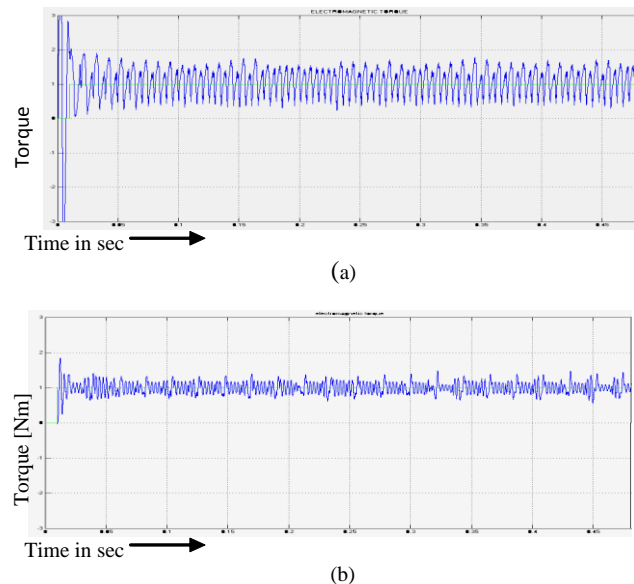


Fig 12: the electromagnetic torque of BLDC motor using Direct Torque control At rated speed (400 rpm), TL=1Nm.

Figure 13 (a) and (b) show the Comparative Result of the electromagnetic torque for both conventional current Control and Direct torque control BLDC at different load condition.

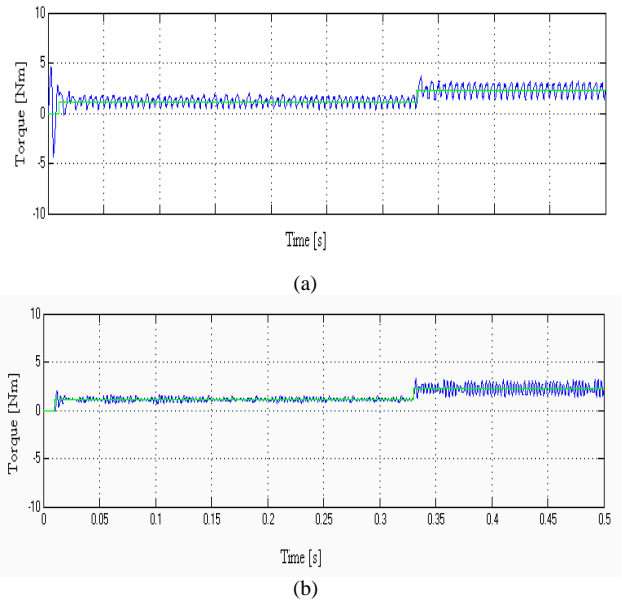


Fig 13: The electromagnetic torque of BLDC motor using Direct Torque control at rated speed (400 rpm), different load condition.

A Comparison of conventional current control and direct torque control given in tabular column which clearly explain that the torque ripple is reduced by 55%.

Table 2: Comparison table

SL.NO	controller	load	Torque ripple (%)
1	Current controller	1Nm	76
		2Nm	72
2	Direct torque controller	1Nm	42
		2Nm	48

## VI. CONCLUSION

This paper concerned the performance of both Conventional Current Control and Direct Torque Control of Brushless Dc motor. In current controlled brushless dc motor the Stator current, the torque and the motor back EMFs are discussed under rated condition. The torque generated by BLDC motor usually has more ripples in conventional current control, nature which leads to speed fluctuation, vibration and acoustic. In Direct Torque Control, on basis of the errors between the reference and the estimated value of flux and torque, it is possible to directly control the inverter states in order to reduce the torque and flux then error with in the pre-fixed band limits.

The simulation results suggest that Direct Torque Control brushless dc motor can be achieve precise control of torque and less steady state error, compared to conventional current control. The simulation was carried out in MATLAB/SIMULINK.

## APPENDIX

### Motor Parameters

The parameters and constants of the BLDC motor drives are shown below

No. of Poles	: 10
No. of Slots	: 12
Rated Speed	: 400 rpm

DC link Voltage (V)	: 36 V
Phase Resistance	: 0.35 ohms
Self-Inductance	: 4.64 mH
Mutual Inductance	: 0.0023 mH
Moment of Inertia	: 0.0002 Kg-m <sup>2</sup>
Friction Co-efficient	: 0.002 Nm/ (rad/sec)
PM excitation flux linkage (wb)	: 0.0794

- [20] M.Arun Noyal Doss, Subhransu Sekar Dash, D.Mahesh, V.Marthandan, "A Model Predictive Control to Reduce Torque Ripple for Brushless DC Motor with Inbuilt Stator Current Control", Universal Journal of Electrical and Electronic Engineering 2013,pp 61-67.

### REFERENCES

- [1] Y. Liu, Z. Q. Zhu, and d. Howe, "Direct Torque Control Of Brushless Dc Drives With Reduced Torque Ripple", IEEE Trans. Ind. Appl., vol. 41, no. 2, pp. 599-608, Mar./Apr. 2005.
- [2] P. J. Sung, W. P. Han, I. H. Man, and f. Harashima, "A New Approach For Minimum-Torque-Ripple Maximum-Efficiency Control of BLDC Motor," IEEE Trans. Ind. Electron., vol. 47, no. 1, pp. 109-114, Feb. 2000.
- [3] C. French and P. Acarnley, "Direct Torque Control Of Permanent Magnet Drives," IEEE Trans. Ind. Appl., vol. 32, no. 5, pp. 1080-1088, Sep./Oct. 1996.
- [4] T. S. Low, K. J. Tseng, K. S. Lock, and K.W. Lim, "Instantaneous Torque Control" In proc. fourth int. conf. Electrical Machines and Drives, pp. 100-105, 13-14 Sep. 1989.
- [5] T. S. Low, K. J. Tseng, T. H. Lee, K. W. Lim, and K. S. Lock, "Strategy for The Instantaneous Torque Control of Permanent - Magnet Brushless Dc Drives", in proc. IEE—elect. Power appl., vol. 137, pp. 355-363, Nov. 1990.
- [6] T. S. Low, T. H. Lee, K. J. Tseng, and K. S. Lock, "Servo Performance of a BLDC Drive With Instantaneous Torque Control," IEEE Trans. Ind. Appl., vol. 28, no. 2, pp. 455-462, Mar./Apr. 1992.
- [7] S. J. Kang and S. K. Sul, "Direct Torque Control Of Brushless Dc Motor With Nonideal Trapezoidal Back - Emf", IEEE Trans. Power electron, vol. 10, no. 6, pp. 796-802, Nov. 1995.
- [9] S. K. Chung, h. S. Kim, C. G. Kim, and M. J. Youn, "A New Instantaneous Torque Control of PM Synchronous Motor for High-Performance Direct-Drive Applications", IEEE Trans. Power electron., vol. 13, no. 3, pp. 388-400, may 1998.
- [10] M. Depenbrock, "Direct Self-Control Of Inverter-Fed Induction Machine", IEEE Trans. Power electron., vol. 3, no. 4, pp. 420-429, Oct. 1988.
- [11] I. Takahashi and T. Noguchi, "A Newquick-Response and High-Efficiency Control Strategies of An Induction Motor", IEEE Trans.. Ind. Appl., vol. 22, no. 5, pp. 820-827, Sep./Oct. 1986.
- [12] L. Zhong, M. F. Rahman, W. Y. Hu, and K. W. Lim, "Analysis of Direct Torque Control in Permanent Magnet Synchronous Motor Drives", IEEE Trans. Power electron. vol. 12, no. 3, pp. 528-536, May 1997.
- [13] Boldea and S. A. Nasar, "Torque Vector Control—A Class of fast and Robust Torque-Speed And Position Digital Controllers For Electric Drives", elect. Mach. Power syst., vol. 15, pp. 135-147, 1988.
- [14] P. C. Krause, "Analysis of Electric Machinery", New York: McGraw- Hill, 1987.
- [15] V. Gourishankar, "Electromechanical Energy Conversion", Scranton, pa: international textbook, 1965. B. H. Ng, M. F. Rahman, and T. S. Low, "An Investigation into the Effects of Machine Parameters on Torque Pulsation in a Brushless Dc Drive," in proc. IEEE iecon '88, pp. 749-754, 1988.
- [16] D. Ishak, Z. Q. Zhu, and D. Howe, "Permanent Magnet Brushless Machines with Unequal Tooth Widths and Similar Slot and Pole Numbers", IEEE Trans. Ind. Appl., vol. 41, no. 2, pp. 584-590, Mar./Apr. 2005.
- [17] F. G. Capponi, g. De donato, I. Del ferraro, o. Honorati, m. C. Harke, and r. D. Lorenz, "Ac Brushless Drive With Low Resolution Hall-Effect Sensors For An Axial Flux Pm Machine," in conf. Rec. 39th IEEE-ias annu. Meeting, oct. 3-7, 2004, pp. 2382-2389.
- [18] R.Goutham Govind Raju, P.Srihari Dattabhimaraju, S.John Pow, S. Mohamed Ali, "Precision motion control using BLDC Motor: Modeling and Control", IJRRES Vol 01, Issue 01; April 2012, pp 52-59.
- [19] R.Goutham Govind Raju, S.John Powl, A.Sathishkumar, P.Sivaprakasam, "Mitigation of Torque for Brushless DC Motor: Modeling and Control", International Journal of Scientific & Engineering Research Volume 3, Issue 5, May-2012.